Theoretical and Applied Climatology
https://doi.org/10.1007/s00704-020-03285-2

ORIGINAL PAPER

Observed changes in heat waves with different severities in China during 1961–2015

Wenxin Xie[1,2] · Botao Zhou[1,2] · Qinglong You[3] · Yuqing Zhang[4] · Safi Ullah[1]

Received: 23 July 2019 / Accepted: 1 June 2020

Abstract
Heat waves (HWs) exert severe impacts on ecosystem, social economy, and human lives. Thus, changes in HWs under a warming climate have triggered extensive interests. In this study, the authors developed a new method to identify the HW events in China by double thresholds and further classified them into four categories (i.e., mild, moderate, severe, and extreme HWs) according to their magnitudes by using the daily maximum temperature data from 701 observation stations. On this basis, the spatiotemporal features of HWs with different severities in China from 1961 to 2015 were investigated. The results show that the high HW frequency mainly appears in Jianghuai, South China and western Northwest China. Moreover, the high frequencies of moderate, severe, and extreme HWs occur from June to August and reach the peak in July, while the mild HW frequency is compared from May to September. Since the 1960s, the frequencies of the mild, moderate, severe, and extreme HWs in China have increased significantly with rates of 7.5, 4.3, 1.4, and 1.8 events per year, respectively. The increases are the greatest in July for the moderate, severe, and extreme HWs while comparable during May to September for the mild HW. Besides, an interdecadal change is found to occur in the late 1990s. Compared with the former period (1961–1996), the occurrence of the extreme HWs during the latter period (1997–2015) has increased most significantly in eastern Northwest China and North China, while the frequency of the mild HWs increases most significantly in Jianghuai and South China.

1 Introduction

Heat wave (HW) is considered as a period of consecutive days with anomalous high temperature. In recent decades, HWs have happened in many regions around the world and resulted in huge economic losses and deaths (e.g., Schär et al. 2004; García-Herrera et al. 2010; Anderson and Bell 2011; Song et al. 2014; Gao et al. 2015; Habeeb et al. 2015; Gu et al. 2016; Xu et al. 2016; Tomczyk and Sulikowska 2018; Williams et al. 2018; Yang et al. 2019). For example, the HW occurring in Europe in 2003 exerted a catastrophic effect on human health and caused excess deaths of more than 70,000 people (Poumadère et al. 2005; Robine et al. 2008; Trigo et al. 2009). A wider and stronger HW event, with the temperature breaking the record, hit central Europe and Russia in 2010 (Barriopedro et al. 2011; Grumm 2011). During the summer time of 2013, eastern China was hit by an unprecedented HW (Xia et al. 2016). In 2017, western and central Europe experienced a mega HW in June (Sánchez-Benítez et al. 2018), and eastern and central China experienced a HW in July, which affected nearly half of the national population (Sparrow et al. 2018). In the late July and early August of 2018, a historically significant HW affected parts of East Asia, with the worst-hit area in Japan (WMO 2019).

Due to severe impacts of HWs, their secular change is of great interest and major concern. So far, there have been a number of studies devoted to changes in HWs over China. It is revealed that there exists a remarkable increase of high temperature in China in recent decades (e.g., Ding et al. 2010; Ding and Qian 2011; Zhou and Ren 2011; Ding and

✉ Botao Zhou
zhoubt@nuist.edu.cn

[1] Key Laboratory of Meteorological Disaster, Ministry of Education (KLME)/Joint International Research Laboratory of Climate and Environmental Change (ILCEC)/Collaborative Innovation Center on Forecast and Evaluation of Meteorological Disasters (CIC-FEMD), Nanjing University of Information Science and Technology, Nanjing 210044, China

[2] School of Atmospheric Sciences, Nanjing University of Information Science and Technology, Nanjing 210044, China

[3] Department of Atmospheric and Oceanic Sciences & Institute of Atmospheric Sciences, Fudan University, Shanghai 200433, China

[4] School of Urban and Environmental Science, Huaiyin Normal University, Huai'an 223300, China

Published online: 14 June 2020

Ke 2015; Zhou et al. 2016; Wang et al. 2017a; You et al. 2017; Shi et al. 2018). Also, the intensity, frequency, and duration of HWs are projected to intensify and exaggerate toward the end of the twenty-first century in a future warmer world (Sun et al. 2014; Zhou et al. 2014; Wang et al. 2015, 2017b; Guo et al. 2017).

Although there are many studies focusing on the spatiotemporal characteristics of HWs, a widely accepted and consistent definition of the HW index has not been established (Meehl and Tebaldi 2004; Xu et al. 2016). Due to different purposes of researches, different HW indices were used. For instance, some indices were defined based on absolute thresholds and some indices based on relative thresholds (Smith et al. 2013; Perkins 2015; Xu et al. 2016; You et al. 2017). For the indices based on absolute thresholds, it is challenging to use them to compare HWs across regions (Russo et al. 2014). The indices defined by relative thresholds may overcome this problem, but most of them capture the HW magnitude only by the number of days exceeding the thresholds (Perkins 2015). Furthermore, only using relative thresholds is hard to distinguish real HWs from normal temperature anomalies particularly in cold regions. Due to this reason, this study attempts to address the characteristics of HWs in different regions of China in a consistent way through constructing a new HW identification by using the relative threshold combined with the absolute threshold. In addition, given that few studies concentrated on the changes in HWs with different severities (i.e., mild, moderate, severe, and extreme) in China, we also examine the spatiotemporal features of mild, moderate, severe, and extreme HWs in China during the last decades in order to provide a fruitful picture for climate change adaptation and mitigation.

2 Data and methods

2.1 Data

The daily maximum temperature (T_{max}) dataset of 768 meteorological stations in China during 1961–2015 is used, which is provided by the China Meteorological Administration (CMA) after quality control, homogeneity testing, and correction processing. Considering the integrity and continuity of the series, stations with the missing data exceeding 31 days were excluded in this study, finally leaving a total of 701 stations for analysis (Fig. 1). For these stations, the missing daily records were filled by the climatological values of daily T_{max} during 1961–2015.

To investigate the characteristics of HWs in sub-regions of China, following You et al. (2017), China is divided into eight sub-regions (Fig. 1a) based on the division of administrative regions and monsoon characteristics.

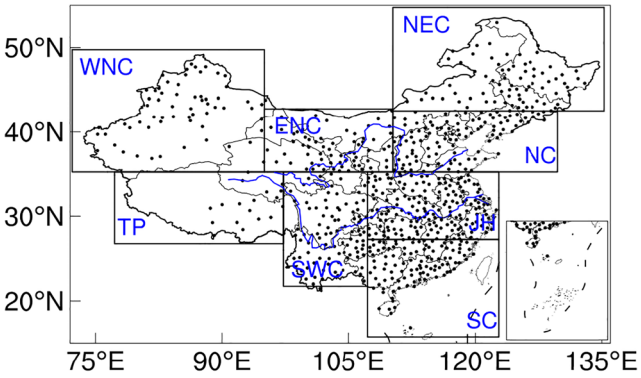

Fig. 1 Distribution of the observation stations, superimposed by the domains of eight sub-regions (NEC—Northeast China, 42.25°–54.75°N/110.25°–135.25°E; NC—North China, 35.25°–42.25°N/110.25°–129.75°E; JH—Jianghuai, 27.25°–35.25°N/107.25°–122.75°E; SC—South China, 15.75°–27.25°N/107.25°–122.75°E; SWC—Southwest China, 21.75°–35.25°N/97.25°–107.25°E; TP—Tibetan Plateau, 26.75°–35.25°N/77.25°–97.25°E; WNC—western Northwest China, 35.25°–49.75°N/72.25°–95°E; ENC—eastern Northwest China, 35.25°–42.75°N/95°–110.25°E)

2.2 Identification of HWs

In the current study, a new HW identification is constructed by both relative threshold and absolute threshold.

The relative threshold at a certain station on day d is the 90th percentile of the set A_d, which is defined as all the T_{max} from $d-15$ days to $d+15$ days in the reference period 1961–1990 as recommended by the Expert Team on Climate Change Detection and Indices (ETCCDI). The set A_d is calculated as:

$$A_d = \bigcup_{y=1961}^{1990} \bigcup_{i=d-15}^{i=d+15} T_{y,i} \quad (1)$$

where $\cup$ is the union of sets and $T_{y,i}$ is the T_{max} on day i in year y. Each station has a corresponding set A_d.

The absolute threshold is defined as the mean of the set B plus one standard deviation. The set B is calculated as:

$$B = \cup_{n=1}^{701} \cup_{y=1961}^{1990} \cup_{i=1}^{153} T_{n,y,i} \quad (2)$$

where $T_{n,y,i}$ denotes the T_{max} on day i in year y at station n. The number 153 indicates the total number of days from May 1 to September 30 when HW events and hot days mainly occur (Ding and Ke 2015; Yang et al. 2019). The number 701 indicates the number of the stations. For a particular target region, there is a specific B value. For the China region, the absolute threshold is 30.9 °C.

If the time period when the T_{max} exceeds both relative and absolute thresholds persists no less than 3 consecutive days, it is considered as one HW event. We have compared the averaged T_{max} of hot days captured by both relative and absolute thresholds with that captured by the relative threshold only. For hot days captured by the relative threshold only, the

averaged T_{max} across the Tibetan Plateau (TP) and some stations in Northeast China (NEC) are below 25 °C, suggesting that even if the temperature in these regions is warmer than the normal, it cannot be regarded as one HW event. Figure 2 shows the daily number of stations with the HWs respectively identified by the relative threshold only and by both relative and absolute thresholds from May to September on the climatology. Compared to that captured by both relative and absolute thresholds, only using the relative threshold overestimates the occurrence of HWs, especially at the start and the end of the summer time. Besides, the HWs based on the relative threshold show little intraseasonal variation, which is consistent with the result of Wang et al. (2017a). However, by considering both relative and absolute thresholds, the intraseasonal variation is yielded. This result demonstrates that taking relative and absolute thresholds together into consideration can distinguish HWs from abnormal temperatures and better display the intraseasonal variation of HWs.

2.3 Classification of HWs with different severities

The magnitude of HWs is calculated based on the HW magnitude index daily (HWMId) method (Russo et al. 2015) in terms of the equation:

$$M_d(T_d) = \begin{cases} \frac{T_d - T_{30y25p}}{T_{30y75p} - T_{30y25p}} & if: T_d > T_{30y25p} \\ 0 & if: T_d \le T_{30y25p} \end{cases} \quad (3)$$

where $T_d$is the T_{max} of hot day d in the HW event; T_{30y25p} and T_{30y75p} are the 25th and 75th percentiles of all the T_{max} in the reference period at a certain station, respectively. M_d is the ratio of the distance from the T_{max} of hot day d in the HW event to the 25th percentile with the interquartile range (IQR). It represents the abnormal excess fraction over the normal excess, and can address climate characteristics in different regions. The sum of M_d for all hot days during one HW event is defined as the HW magnitude in this study. This index can simultaneously measure the duration and the intensity of HW, which has been applied in several studies to examine the observed and projected changes of HWs in Africa and Europe (Zampieri et al. 2016; Russo et al. 2015, 2016; Dosio 2017; Sánchez-Benítez et al. 2018).

Based on the magnitude, we classified the HWs into four categories: the mild, moderate, severe, and extreme HWs, to describe their severities. Specifically, we firstly counted the number of HW events over a fixed threshold (HWMId magnitude) at each station of China for the period 1961–2015. Then, the percentage of stations that experience at least one HW event over a fixed threshold (HWMId magnitude) was calculated. According to the skewed distribution of the station percentage, the severity of HWs was determined. Figure 3 presents the statistic result of station percentage corresponding to different magnitudes. On average, there are about 62%, 40%, 20%, and 10% of stations in which at least one HW event with HWMId > 0, HWMId > 6, HWMId > 9, and HWMId > 12 occurred, respectively. Following Fig. 3, we defined the events with 0 < HWMId ≤ 6, 6 < HWMId ≤ 9, 9 < HWMId ≤ 12, and HWMId > 12 as the mild, moderate, severe, and extreme HWs, respectively, in this study. This selection for the classification of HWs is in accord with Russo et al. (2014) and can be further justified by the empirical cumulative distribution function (CDF) of the magnitudes of all HWs in China during 1961–2015. As shown in Fig. 4, the cumulative probabilities corresponding to the HWMId magnitudes of 6, 9, and 12 are in turn 0.56, 0.83, and 0.92, representing the conditions of half, most, and almost all of the HW events. Namely, the occurrence of mild, moderate, severe, and extreme HW events corresponds to a probability of 56%, 27%, 9%, and 8%, respectively.

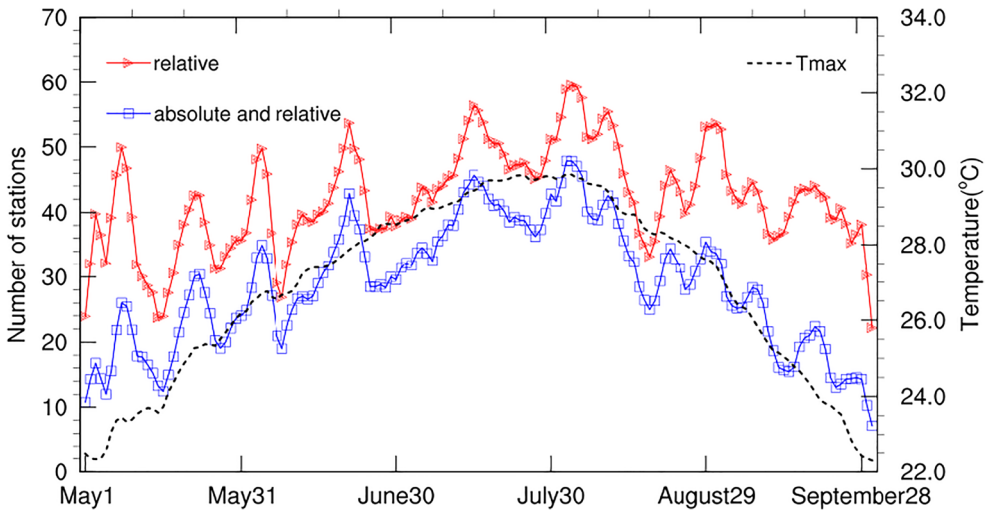

Fig. 2 Daily mean T_{max} (black line) and daily number of stations with HW events as identified by absolute and relative thresholds (blue line) and only by relative threshold (red line) from May to September during 1961–2015

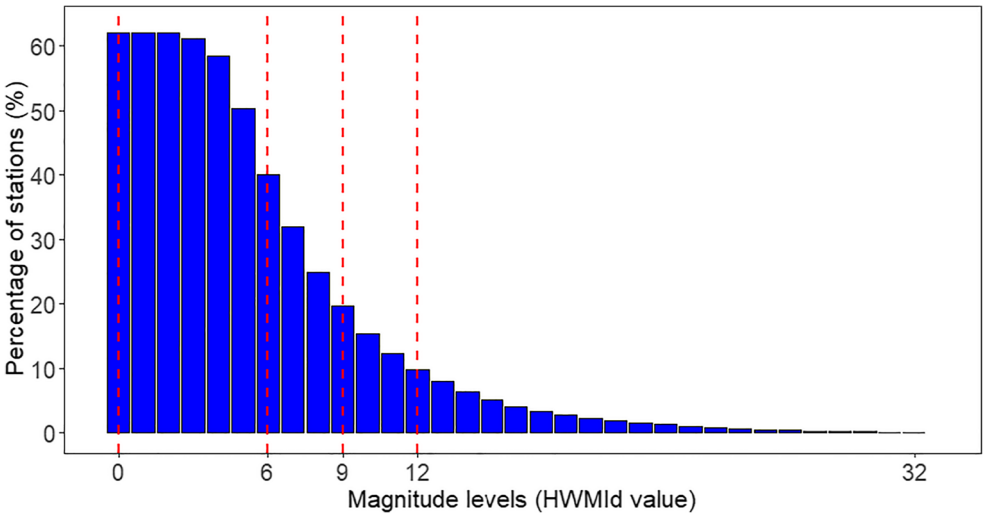

Fig. 3 Percentage of stations (ordinate) where at least one HW event is detected over a fixed threshold (abscissa)

2.4 Statistical methods

In this study, Sen's slope method (Sen 1968), as a robust nonparameter method, is used to calculate trends. The significance of trends is determined by the modified Mann–Kendall (MM-K) test. This test can solve the problem of series auto-correlation that exists in the traditional nonparametric Mann–Kendall (M-K) test (Hamed and Rao 1998). Because both of the MM-K and Sen's slope methods are nonparametric and less sensitive to extreme values, these methods are well suited for estimating the slope of climate extreme metrics and testing their trend significance (Zhang et al. 2012; Panda et al. 2017; Lin et al. 2018). The Wilcoxon rank sum test (Wilcoxon 1945), which is also a nonparametric method, is applied to assess the significance of differences between two sub-periods. Besides, the Cramér–von Mises (CvM) test, which can test the difference between two independent, identically distributed time series and detect the mutation point of univariate time series (Holmes et al. 2013; Mazdiyasni and AghaKouchak 2015; Sharma and Mujumdar 2017), is further employed for mutation point analysis.

3 Results

Figure 5 displays the spatial distribution of the HW frequency and magnitude averaged over the course of 1961–2015. It can be clearly observed that the stations with the HW frequency higher than 2 events per year are mainly located in Jianghuai (JH), South China (SC), and western Northwest China (WNC). The number of HWs in NEC is generally less than 1.5 events per year, indicating relatively less frequency of HWs there (Fig. 5a). The mean HW magnitude is relatively smaller in the regions with high HW frequency, especially in the central part of southeastern China. In contrast, the HW magnitude is relatively larger in the regions with low HW frequency, for instance, in Yunnan Province located in

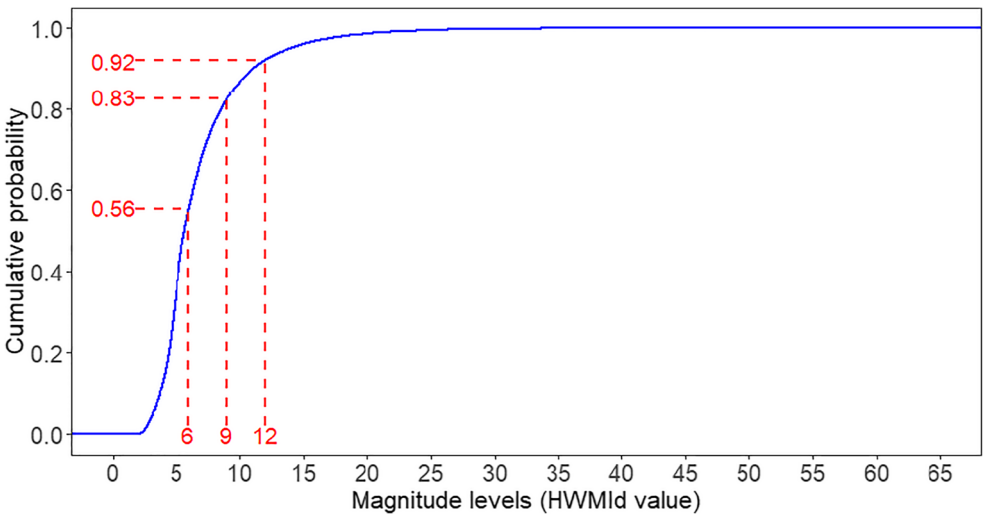

Fig. 4 Empirical cumulative distribution function (CDF) of HW events during 1961–2015. The abscissa denotes HW magnitude and the ordinate indicates cumulative probability

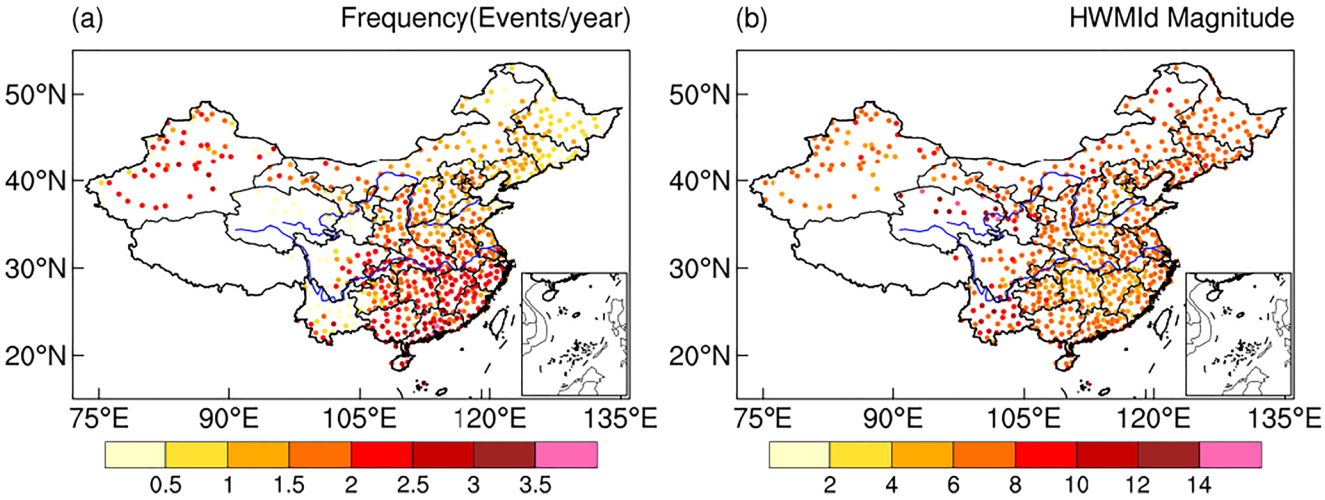

Fig. 5 Spatial distribution of (**a**) HW frequency and (**b**) HWMId magnitude averaged over 1961–2015

Southwest China (SWC) and Qinghai Province located in eastern Northwest China (ENC) (Fig. 5b).

The climatological distribution of the frequency of different categories of HWs across China is shown in Fig. 6. It indicates that the spatial patterns of severe and extreme HWs are spatially more homogenous than those of mild and moderate HWs. Especially, the middle reaches of the Yangtze River valley, which experience more mild and moderate

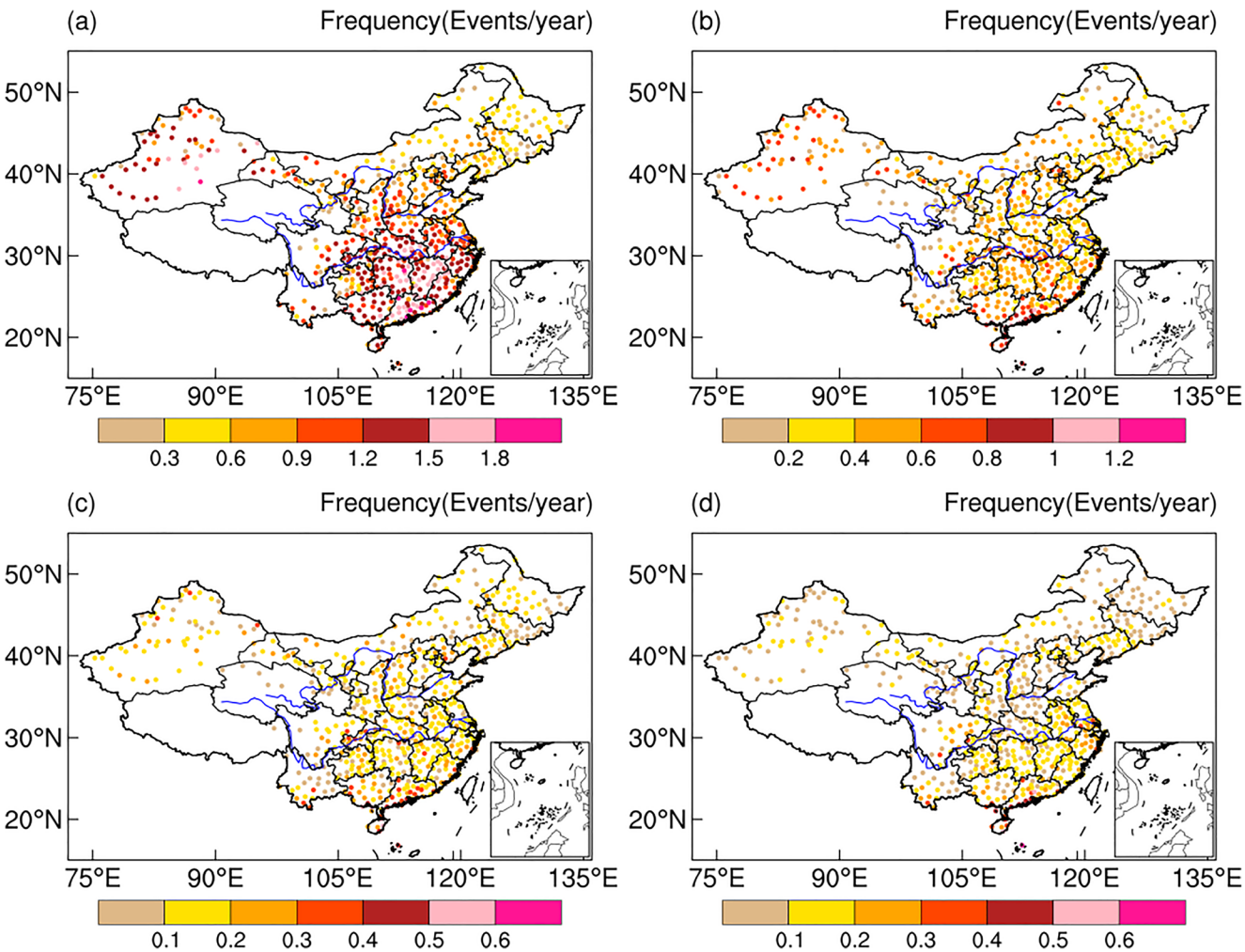

Fig. 6 Spatial distribution of the frequencies of (**a**) mild, (**b**) moderate, (**c**) severe, and (**d**) extreme HWs averaged over 1961–2015

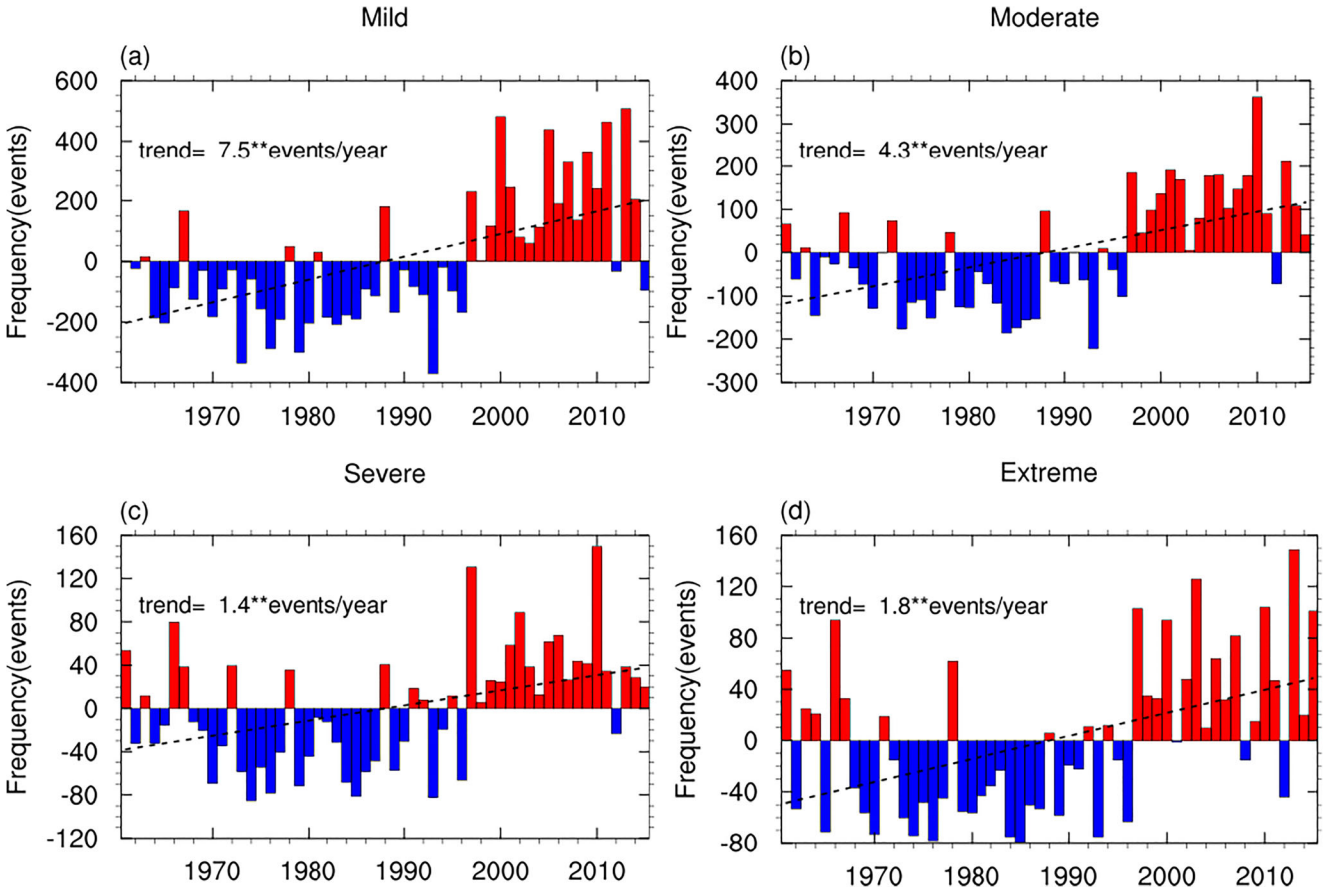

Fig. 7 Temporal variations (bar) and linear trends (dashed line) of anomalies in the total frequencies of (**a**) mild, (**b**) moderate, (**c**) severe, and (**d**) extreme HWs during 1961–2015 over all the stations. ** denotes the trends significant at the 0.01 confidence level

HWs, are affected by fewer severe and extreme HWs, as compared to the lower reaches of the Yangtze River valley. Being the sub-regions with the highest occurrence of HWs, SC encounters mild, moderate, severe, and extreme HWs with the frequencies of 1.28, 0.59, 0.21, and 0.20 events per year on average, respectively; the counterparts for JH are 1.14, 0.44, 0.15, and 0.14 events per year, respectively. In WNC, the frequencies of mild and moderate HWs are respectively 0.91 and 0.47 events per year, while the frequencies of severe and extreme HWs are close to those in other sub-regions (except JH and SC) and even less than those in North China (NC). On the national average, the frequencies are 0.81, 0.40, 0.14, and 0.11 events per year for mild, moderate, severe, and extreme HWs, respectively.

The general features that the HW magnitude is smaller (larger) in the regions with high (low) HW frequency and the spatial distribution of severe and extreme HWs is more homogenous are related to the consideration of double thresholds, especially the absolute threshold in our definition for the identification of HW events, which lies at the lower threshold for the climatological warm regions but at the higher threshold for the climatological cold regions. Compared with the previous studies, our finding generally agrees with the result based on the HW definition by the fixed threshold that the high frequency of HWs is mainly located in eastern China and northwestern China (e.g., Ding et al. 2010; Wang et al. 2017a). However, due to the set of double thresholds in our definition, a more distinct spatial variation is shown and the frequencies in NEC and ENW are comparatively higher.

Figure 7 shows the temporal variations of the frequencies of mild, moderate, severe, and extreme HWs over China from 1961 to 2015. An overall increasing trend is explicitly observed for all the four categories. During 1961–2015, the increasing rates related to the mild, moderate, severe, and extreme HWs are 7.5, 4.3, 1.4, and 1.8 events per year, respectively. They are all significant at the 0.01 confidence level.

In addition to the trend, an interdecadal change in the late 1990s for the four categories of HWs can also be noticed from Fig. 7, which have previously been in a negative phase before that time and then progressed into a positive one. The CvM test for mutation point demonstrates that the maximum differences appear in 1997 (Fig. 8). Their differences for the periods after and before 1997 are also significant at the 0.05 confidence level as calculated from the Wilcoxon rank sum test.

The increasing trend of HWs and similar decadal shift in the 1990s have been previously reported in some studies (e.g.,

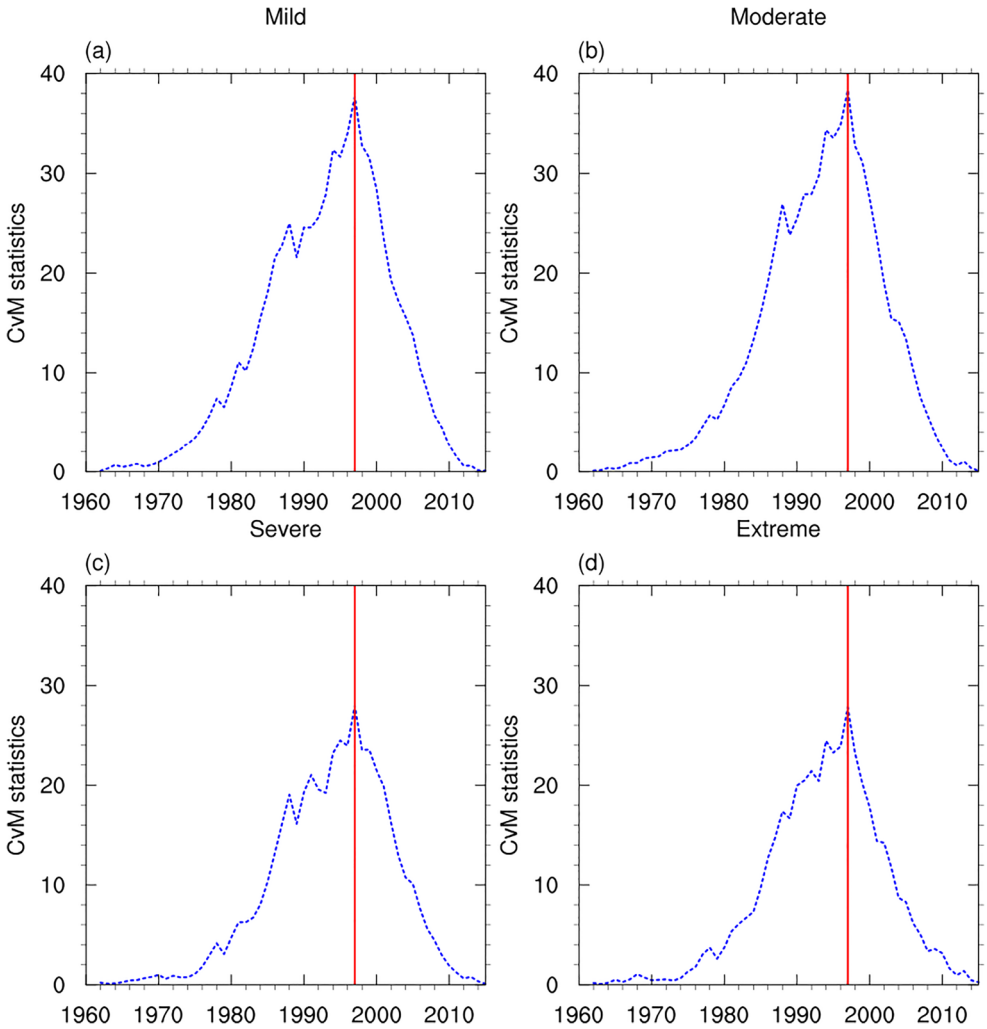

Fig. 8 The CvM statistics for (**a**) mild, (**b**) moderate, (**c**) severe, and (**d**) extreme HWs over China during 1961–2015. The red vertical line shows the position of the maximum CvM statistic value

Qi and Wang 2012; Ding and Ke 2015; Lu and Chen 2016; Zhou et al. 2016; You et al. 2017). However, different from the previous studies focusing on a single aspect of HWs, our study provides the changes of HWs with different severities, through the classification of HWs based on the HWMId magnitude which takes into account both duration and intensity of HWs.

Table 1 further summarizes the frequencies of the four categories of HWs during different time periods. The percentages of stations affected by each type of HWs were also estimated to evaluate their influential extent. As presented in the table, all the four categories of HWs occur more frequently in the 1960s and then decline in both the 1970s and the 1980s. After the 1990s, their frequencies and influential extents increase significantly and reach the highest point after the beginning of the twenty-first century. Relative to the period of 1961–1996, both the frequency and the extent of the four categories of HWs increase remarkably during the period 1997–2015 and almost double for the moderate,

Table 1 Extent (%) and frequency (shown in the parentheses) of different categories of HWs in China for different time periods

HWs	1961–1970	1971–1980	1981–1990	1990–2000	2001–2015	1961–1996	1997–2015
Mild	45.2 (504)	39.1 (410)	43.6 (475)	48.8 (568)	56.4 (787)	42.3 (457)	57.3 (785)
Moderate	27.8 (248)	23.3 (202)	21.4 (185)	30.2 (284)	40.3 (410)	24.2 (211)	40.0 (407)
Severe	12.5 (99)	7.9 (59)	8.2 (63)	13.0 (104)	17.4 (144)	9.6 (74)	17.4 (144)
Extreme	9.5 (74)	5.9 (45)	4.8 (37)	11.6 (91)	15.0 (129)	6.8 (52)	15.6 (133)

The frequency is counted as the number of events over all the stations

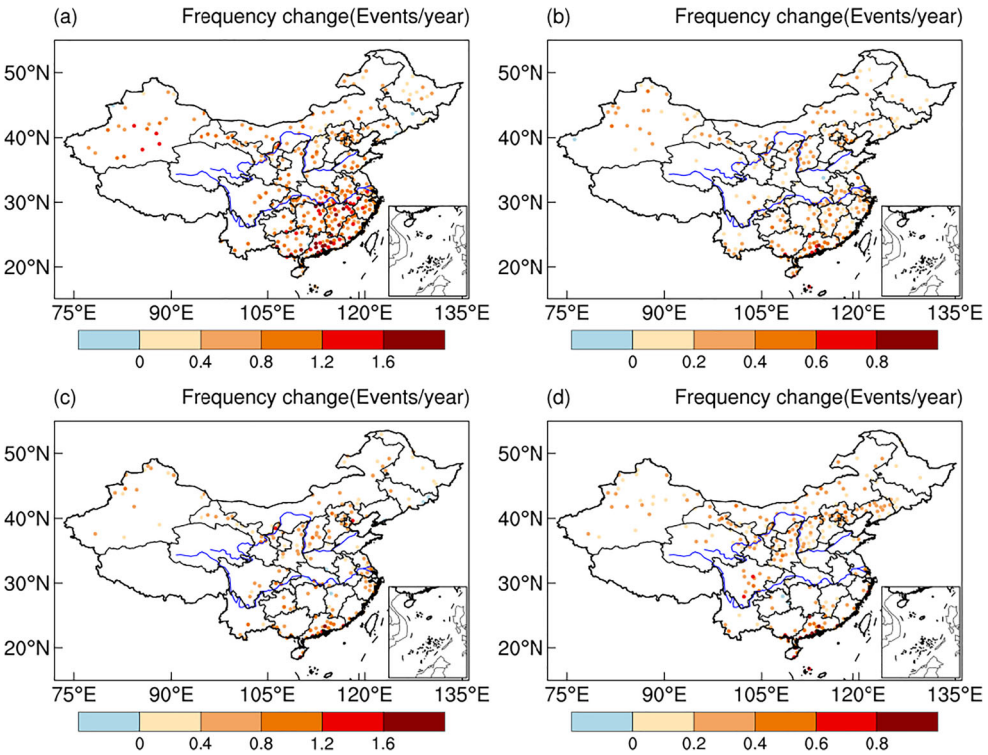

Fig. 9 Difference of the frequencies of (**a**) mild, (**b**) moderate, (**c**) severe, and (**d**) extreme HWs between 1997 and 2015 and 1961–1996. Only the stations with difference significant at the 0.1 confidence level are shown

severe, and extreme HWs. The Wilcoxon rank sum test indicates that these increases are significant at the 0.05 confidence level.

To investigate the spatial difference of the interdecadal change in the frequencies of the four categories of HWs, their anomalies between 1997 and 2015 and 1961–1996 are plotted (Fig. 9). With respect to the period 1961–1996, the frequency of mild HWs increases over most of China. As the severity of HWs increases, the number of stations with significant changes is decreased. This is particularly evident in SC and JH. As shown in Table 2, in these two sub-regions, 73% and 55% of stations show significant increases in mild HWs while only 39% and 13% of stations show significant increases in extreme HWs, respectively. In contrast, the extreme HWs increase significantly in ENC and NC (Fig. 9d). For these two sub-regions, the significant increases in extreme HWs are detected over 74% and 57% of stations, respectively (Table 2).

We also explored the intraseasonal variations of HWs in China with different severities. Considering some HW processes may cut across either the beginning or the end of a month, the total number of hot days for the period of 1961–2015 involved in each type of HWs in a given month was estimated. As shown in Fig. 10, the number of hot days affiliated in mild HW events varies from 24.7 to 32.5 days/station in hot season, implying that the mild HWs occur with high frequency in all the five months. For moderate, severe, and extreme HWs, the large number of hot days mainly appears in June to August and reaches the peak in July. Moreover, the hot days within the extreme HWs in July and August are even higher than that for the severe HWs. The intraseasonal variation of the extent, which was defined as the percentage of the stations covered by HWs to the total stations, is generally consistent with the result for hot days.

Figure 11 shows the trend of the total number and the extent of hot days for different categories of HWs in each

Table 2 Percentage (%) of stations with significant changes between 1997 and 2015 and 1961–1996 for different categories of HWs over the sub-regions of China and their respective frequencies (shown in the parentheses) during 1961–1996 and 1997–2015

HWs	NEC	NC	JH	SC	SWC	WNW	ENW
Mild	34 (30/52)	47 (49/82)	55 (162/270)	73 (103/193)	24 (38/62)	34 (48/72)	48 (24/51)
Moderate	31 (20/40)	37 (29/55)	38 (61/107)	60 (43/98)	22 (20/36)	37 (24/38)	42 (14/33)
Severe	24 (7/14)	31 (9/23)	19 (24/34)	30 (16/35)	14 (7/14)	26 (6/12)	35 (4/13)
Extreme	29 (3/10)	57 (3/19)	13 (23/27)	39 (13/37)	23 (5/16)	39 (3/8)	74 (2/15)

The frequency is counted as the number of events over all the stations of the sub-regions

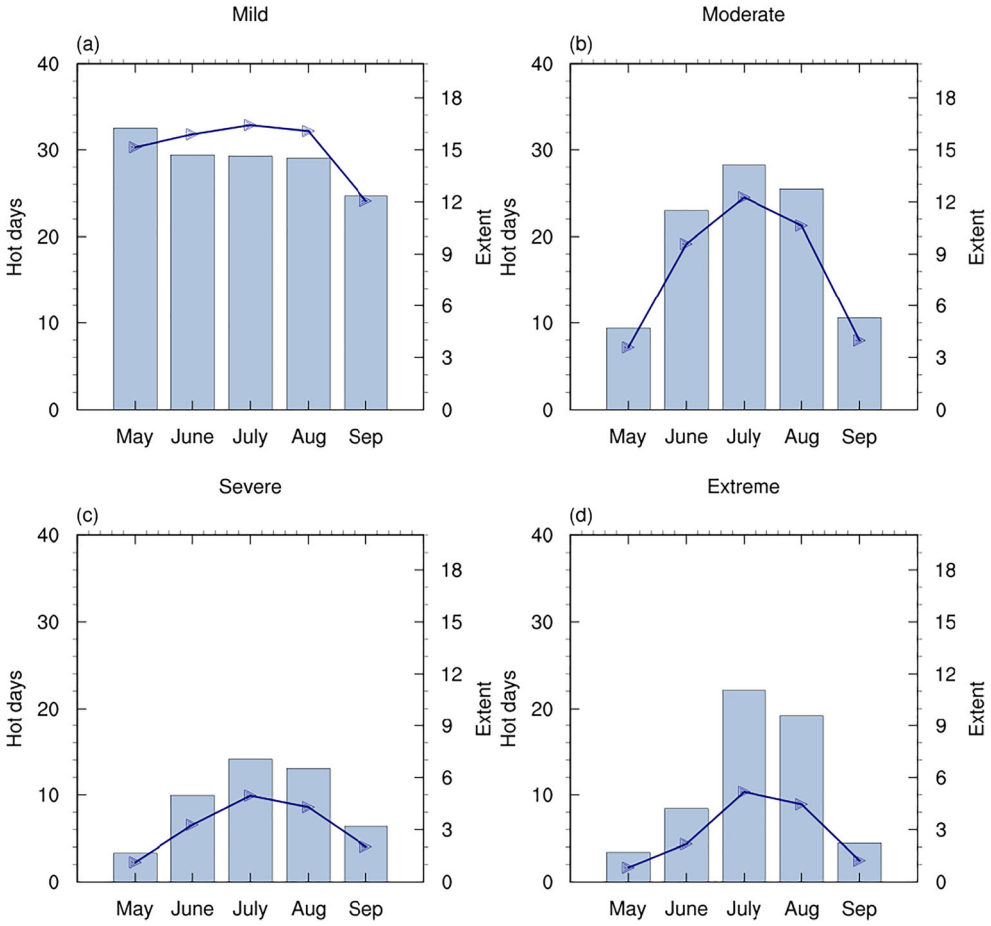

Fig. 10 Monthly hot days (days/station, bar) and extent (%, line) of (**a**) mild, (**b**) moderate, (**c**) severe, and (**d**) extreme HWs in May to September during 1961–2015. The number of hot days is shown as the total days in 55 years divided by the station number. The extent is for the average of each year

month of hot season. Note that the total number of hot days for each month of a year was counted as the sum of hot days over all the stations. Seen from this figure, we can also notice the pronounced intraseasonal differences in trend change for each category of HWs. For the mild HWs, the increasing trends are comparable among each month. However, for the moderate, severe, and extreme HWs, the number of hot days increases sharply in the months when relatively more HWs occur. The total hot days over all the stations increase the most in July with the increasing trends of 5.5, 3.6, and 5.2 days per year for moderate, severe, and extreme HWs, respectively.

4 Summary and discussion

In this study, based on the observed daily T_{max} during 1961–2015 at 701 stations in China, we developed a new method to identify the HWs in China by the combination of absolute and relative thresholds. Our results show a better representation for the HWs in China by using the combination of absolute and relative thresholds as compared to that only using the relative threshold or the absolute threshold.

On the above basis, we further calculated the HW magnitude by using the HWMId method. The HWMId sums the excess of T_{max} beyond a certain normalized threshold in a given period, and merges the duration and the intensity of HWs into a quantitative value. It thus enables the comparison of HWs with different length and peak magnitudes that occur in different regions and different time periods (Russo et al. 2014, 2015). According to their magnitudes and based on the station percentages as well as cumulative probabilities of all HWs occurring in China during 1961–2015, we set up a criteria to classify the HWs into four categories, i.e., mild, moderate, severe, and extreme HWs. The spatiotemporal features of the four categories of the HWs in the past 55 years were then examined in order to provide more detailed and comprehensive information for the adaptation to climate extremes. The major findings obtained from this study are summarized as follows:

1. Climatologically, the high HW frequencies mainly occur in JH, SC, and WNC. The frequencies of severe and extreme HWs are spatially more homogenous than those of mild and moderate HWs. On the national average, the frequencies for mild, moderate, severe, and extreme HWs are 0.81, 0.40, 0.14, and 0.11 events per year, respectively. In addition, the moderate, severe, and extreme HWs show evident intraseasonal variations, with high

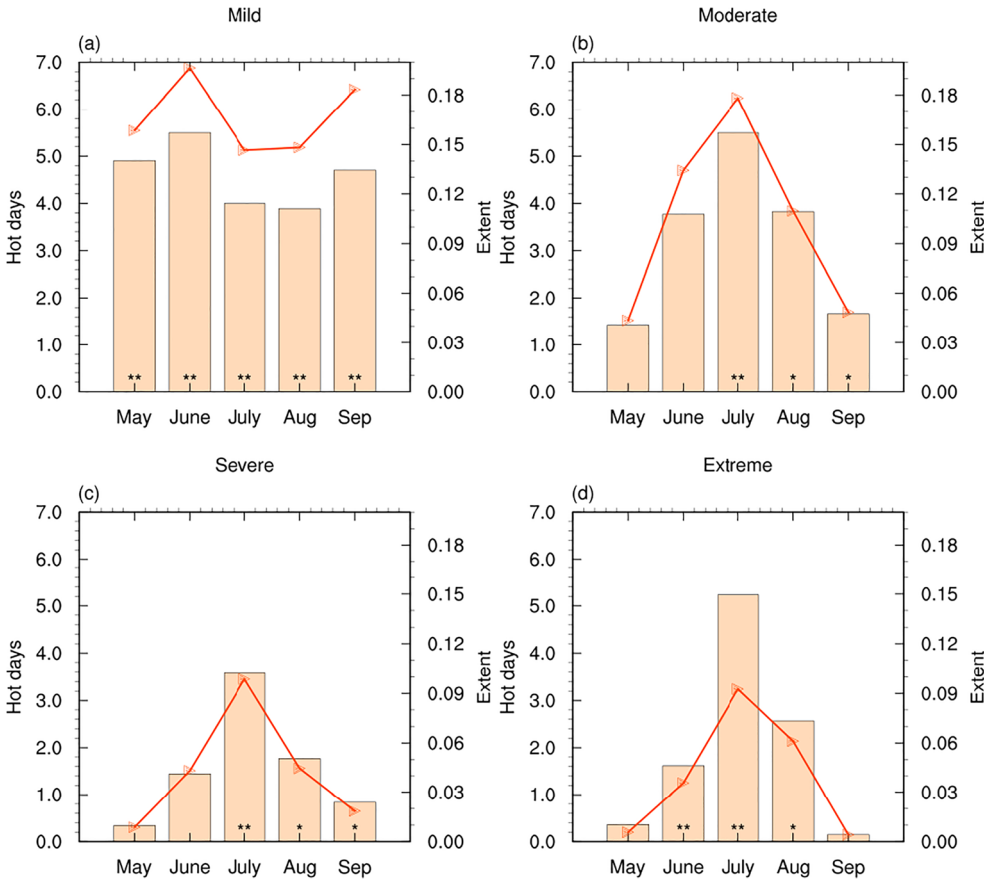

Fig. 11 Trends of hot days (days/year, bar) and extent (%/year, line) of (**a**) mild, (**b**) moderate, (**c**) severe, and (**d**) extreme HWs in May to September during 1961–2015. The trends were calculated based on the series of hot day number in all stations in each year. * and ** denote the trends of hot days significant at the 0.05 and 0.01 confidence level, respectively

frequencies appearing during June to August and reaching the peak in July. Nevertheless, the frequency of mild HWs is compared from May to September.

2. Since the 1960s, the frequencies of mild, moderate, severe, and extreme HWs over China have increased significantly, with the rates of 7.5, 4.3, 1.4, and 1.8 events per year, respectively. The increases are the greatest in July for moderate, severe, and extreme HWs while comparable during May to September for mild HWs.
3. There exists an evident interdecadal difference in mild, moderate, severe, and extreme HWs before and after the late 1990s. Relative to the former sub-period, the frequency of the four categories of HWs increases significantly in the latter sub-period and almost doubles for moderate, severe, and extreme HWs. Spatially, the occurrence of extreme HWs during the latter period has increased most in ENC and NC, while the frequency of mild HWs increases most in JC and SC.

It should be noted that this study just focused on the observed changes of the HWs in China with different severities. The physical causes for their changes are not addressed. Some studies have highlighted that changes in sea surface temperature, soil moisture, snow cover, solar irradiance, and greenhouse gases play important roles in the change of HWs (Fischer et al. 2007; Wu et al. 2012; Sun et al. 2014; Chen and Zhou 2018; Wang et al. 2017a; Sparrow et al. 2018; Chen et al. 2019a, b). The urbanization has also been documented to exert a significant effect. It may advance the timing of the onset of HWs, and help the HWs become more frequent, more intense, and longer lasting (Luo and Lau 2017; Lin et al. 2018). And the urban heat island is also related to the HW magnitude (Herbel et al. 2018). However, the detailed physical mechanisms responsible for the behaviors of different categories of HWs in different regions may be rather complicated, which deserves further in-depth investigation in the future studies in order to get a full picture for the understanding of the change in HWs.

Acknowledgments This research was jointly supported by the National Key Research and Development Program of China (2018YFA0606301 and 2016YFA0600701), the National Natural Science Foundation of China (41991285 and 41675069), the Startup Foundation for Introducing Talent of NUIST (2018r060), and the National Program for Support of Top-notch Young Professionals.

References

Anderson GB, Bell ML (2011) Heat waves in the United States: mortality risk during heat waves and effect modification by heat wave characteristics in 43 U.S. communities. Environ Health Perspect 119(2): 210–218. https://doi.org/10.1289/ehp.1002313

Barriopedro D, Fischer EM, Luterbacher J, Trigo RM, García-Herrera R (2011) The hot summer of 2010: redrawing the temperature record map of Europe. Science 332(6026):220–224. https://doi.org/10.1126/science.1201224

Chen X, Zhou T (2018) Relative contributions of external SST forcing and internal atmospheric variability to July–August heat waves over the Yangtze River valley. Clim Dyn 51(11–12):4403–4419. https://doi.org/10.1007/s00382-017-3871-y

Chen R, Wen Z, Lu R (2019a) Influences of tropical circulation and sea surface temperature anomalies on extreme heat over Northeast Asia in the midsummer of 2018. Atmos Ocean Sci Lett 12(4):238–245. https://doi.org/10.1080/16742834.2019.1611170

Chen R, Wen Z, Lu R, Wang C (2019b) Causes of the extreme hot midsummer in central and South China during 2017: role of the western tropical Pacific warming. Adv Atmos Sci 36(5):465–478. https://doi.org/10.1007/s00376-018-8177-4

Ding T, Ke Z (2015) Characteristics and changes of regional wet and dry heat wave events in China during 1960–2013. Theor Appl Climatol 122(3–4):651–665. https://doi.org/10.1007/s00704-014-1322-9

Ding T, Qian W (2011) Geographical patterns and temporal variations of regional dry and wet heatwave events in China during 1960–2008. Adv Atmos Sci 28(2):322–337. https://doi.org/10.1007/s00376-010-9236-7

Ding T, Qian W, Yan Z (2010) Changes in hot days and heat waves in China during 1961–2007. Int J Climatol 30(10):1452–1462. https://doi.org/10.1002/joc.1989

Dosio A (2017) Projection of temperature and heat waves for Africa with an ensemble of CORDEX regional climate models. Clim Dyn 49: 493–519. https://doi.org/10.1007/s00382-016-3355-5

Fischer EM, Seneviratne SI, Vidale PL, Vüthi D, Schär C (2007) Soil moisture–atmosphere interactions during the 2003 European summer heat wave. J Clim 20(20):5081–5099. https://doi.org/10.1175/JCLI4288.1

Gao J, Sun Y, Liu Q, Zhou M, Lu Y, Li L (2015) Impact of extreme high temperature on mortality and regional level definition of heat wave: a multi-city study in China. Sci Total Environ 505:535–544. https://doi.org/10.1016/j.scitotenv.2014.10.028

García-Herrera R, Díaz J, Trigo RM, Luterbacher J, Fischer EM (2010) A review of the European summer heat wave of 2003. Crit Rev Environ Sci Technol 40(4):267–306. https://doi.org/10.1080/10643380802238137

Grumm RH (2011) The central European and Russian heat event of July–August 2010. Bull Am Meteorol Soc 92(10):1285–1296. https://doi.org/10.1175/2011BAMS3174.1

Gu S, Huang C, Bai L, Chu C, Liu Q (2016) Heat-related illness in China, summer of 2013. Int J Biometeorol 60(1):131–137. https://doi.org/10.1007/s00484-015-1011-0

Guo X, Huang J, Luo Y, Zhao Z, Xu Y (2017) Projection of heat waves over China for eight different global warming targets using 12 CMIP5 models. Theor Appl Climatol 128(3–4):507–522. https://doi.org/10.1007/s00704-015-1718-1

Habeeb D, Vargo J, Stone B (2015) Rising heat wave trends in large US cities. Nat Hazards 76(3):1651–1665. https://doi.org/10.1007/s11069-014-1563-z

Hamed KH, Rao AR (1998) A modified Mann–Kendall trend test for autocorrelated data. J Hydrol 204(1–4):182–196. https://doi.org/10.1016/S0022-1694(97)00125-X

Herbel I, Croitoru A-E, Rus AV, Roşca CF, Harpa GV, Ciupertea A-F, Rus I (2018) The impact of heat waves on surface urban heat island and local economy in Cluj-Napoca city, Romania. Theor Appl Climatol 133(3–4):681–695. https://doi.org/10.1007/s00704-017-2196-4

Holmes M, Kojadinovic I, Quessy J-F (2013) Nonparametric tests for change-point detection à la Gombay and Horváth. J Multivar Anal 115:16–32. https://doi.org/10.1016/j.jmva.2012.10.004

Lin L, Ge E, Liu X, Liao W, Luo M (2018) Urbanization effects on heat waves in Fujian Province, Southeast China. Atmos Res 210:123–132. https://doi.org/10.1016/j.atmosres.2018.04.011

Lu R, Chen R (2016) A review of recent studies on extreme heat in China. Atmos Ocean Sci Lett 9:114–121. https://doi.org/10.1080/16742834.2016.1133071

Luo M, Lau N-C (2017) Heat waves in southern China: synoptic behavior, long-term change, and urbanization effects. J Clim 30(2):703–720. https://doi.org/10.1175/JCLI-D-16-0269.1

Mazdiyasni O, AghaKouchak A (2015) Substantial increase in concurrent droughts and heatwaves in the United States. Proc Natl Acad Sci 112(37):11484–11489. https://doi.org/10.1073/pnas.1422945112

Meehl GA, Tebaldi C (2004) More intense, more frequent, and longer lasting heat waves in the 21st century. Science 305(5686):994–997. https://doi.org/10.1126/science.1098704

Panda DK, AghaKouchak A, Ambast SK (2017) Increasing heat waves and warm spells in India, observed from a multiaspect framework. J Geophys Res Atmos 122(7):3837–3858. https://doi.org/10.1002/2016JD026292

Perkins SE (2015) A review on the scientific understanding of heatwaves—their measurement, driving mechanisms, and changes at the global scale. Atmos Res 164–165:242–267. https://doi.org/10.1016/j.atmosres.2015.05.014

Poumadère M, Mays C, Le Mer S, Blong R (2005) The 2003 heat wave in France: dangerous climate change here and now. Risk Anal 25(6): 1483–1494. https://doi.org/10.1111/j.1539-6924.2005.00694.x

Qi L, Wang Y (2012) Changes in the observed trends in extreme temperatures over China around 1990. J Clim 25(15):5208–5222. https://doi.org/10.1175/JCLI-D-11-00437.1

Robine J-M, Cheung SLK, Le Roy S, Van Oyen H, Griffiths C, Michel J-P, Herrmann FR (2008) Death toll exceeded 70,000 in Europe during the summer of 2003. C R Biol 331(2):171–178. https://doi.org/10.1016/j.crvi.2007.12.001

Russo S, Dosio A, Graversen RG, Sillmann J, Carrao H, Dunbar MB, Singleton A, Montagna P, Barbola P, Vogt JV (2014) Magnitude of extreme heat waves in present climate and their projection in a warming world. J Geophys Res 119(22):12500–12512. https://doi.org/10.1002/2014JD022098

Russo S, Sillmann J, Fischer EM (2015) Top ten European heatwaves since 1950 and their occurrence in the coming decades. Environ Res Lett 10(12):124003. https://doi.org/10.1088/1748-9326/10/12/124003

Russo S, Marchese AF, Sillmann J, Immé G (2016) When will unusual heat waves become normal in a warming Africa? Environ Res Lett 11:054016. https://doi.org/10.1088/1748-9326/11/5/054016

Sánchez-Benítez A, García-Herrera R, Barriopedro D, Sousa PM, Trigo RM (2018) June 2017: the earliest European summer mega-heatwave of reanalysis period. Geophys Res Lett 45(4):1955–1962. https://doi.org/10.1002/2018GL077253

Schär C, Vidale PL, Lüthi D, Frei C, Häberli C, Liniger MA, Appenzeller C (2004) The role of increasing temperature variability in European

summer heatwaves. Nature 427(6972):332–336. https://doi.org/10.1038/nature02300

Sen PK (1968) Estimates of the regression coefficient based on Kendall's tau. J Am Stat Assoc 63(324):1379–1389. https://doi.org/10.1080/01621459.1968.10480934

Sharma S, Mujumdar P (2017) Increasing frequency and spatial extent of concurrent meteorological droughts and heatwaves in India. Sci Rep 7:15582. https://doi.org/10.1038/s41598-017-15896-3

Shi J, Cui L, Ma Y, Du H, Wen K (2018) Trends in temperature extremes and their association with circulation patterns in China during 1961–2015. Atmos Res 212:259–272. https://doi.org/10.1016/j.atmosres.2018.05.024

Smith TT, Zaitchik BF, Gohlke JM (2013) Heat waves in the United States: definitions, patterns and trends. Clim Chang 118(3–4):811–825. https://doi.org/10.1007/s10584-012-0659-2

Song X, Zhang Z, Chen Y, Wang P, Xiang M, Shi P, Tao F (2014) Spatiotemporal changes of global extreme temperature events (ETEs) since 1981 and the meteorological causes. Nat Hazards 70(2):975–994. https://doi.org/10.1007/s11069-013-0856-y

Sparrow S, Su Q, Tian F, Li S, Chen Y, Chen W, Luo F, Freychet N, Lott FC, Dong B, Tett SFB, Wallom D (2018) Attributing human influence on the July 2017 Chinese heatwave: the influence of sea-surface temperatures. Environ Res Lett 13(11):114004. https://doi.org/10.1088/1748-9326/aae356

Sun Y, Zhang X, Zwiers FW, Song L, Wan H, Hu T, Yin H, Ren G (2014) Rapid increase in the risk of extreme summer heat in eastern China. Nat Clim Chang 4(12):1082–1085. https://doi.org/10.1038/nclimate2410

Tomczyk AM, Sulikowska A (2018) Heat waves in lowland Germany and their circulation-related conditions. Meteorog Atmos Phys 130(5):499–515. https://doi.org/10.1007/s00703-017-0549-2

Trigo RM, Ramos AM, Nogueira PJ, Santos FD, Garcia-herrera R, Gouveia C, Santo FE (2009) Evaluating the impact of extreme temperature based indices in the 2003 heatwave excessive mortality in Portugal. Environ Sci Pol 12(7):844–854. https://doi.org/10.1016/j.envsci.2009.07.007

Wang W, Zhou W, Li Y, Wang X, Wang D (2015) Statistical modeling and CMIP5 simulations of hot spell changes in China. Clim Dyn 44(9–10):2859–2872. https://doi.org/10.1007/s00382-014-2287-1

Wang P, Tang J, Sun X, Wang S, Wu J, Dong X, Fang J (2017a) Heat waves in China: definitions, leading patterns, and connections to large-scale atmospheric circulation and SSTs. J Geophys Res Atmos 122(20):10679–10699. https://doi.org/10.1002/2017JD027180

Wang Y, Zhou B, Qin D, Wu J, Gao R, Song L (2017b) Changes in mean and extreme temperature and precipitation over the arid region of northwestern China: observation and projection. Adv Atmos Sci 34(3):289–305. https://doi.org/10.1007/s00376-016-6160-5

Wilcoxon F (1945) Individual comparisons by ranking methods. Biom Bull 1(6):80–83. https://doi.org/10.2307/3001968

Williams S, Venugopal K, Nitschke M, Nairn J, Fawcett R, Beattie C, Wynwood G, Bi P (2018) Regional morbidity and mortality during heatwaves in South Australia. Int J Biometeorol 62(10):1911–1926. https://doi.org/10.1007/s00484-018-1593-4

WMO (2019) WMO Statement on the State of the Global Climate in 2018. WMO-No. 1233, World Meteorological Organization

Wu Z, Jiang Z, Li J, Zhong S, Wang L (2012) Possible association of the western Tibetan plateau snow cover with the decadal to interdecadal variations of northern China heatwave frequency. Clim Dyn 39(9–10):2393–2402. https://doi.org/10.1007/s00382-012-1439-4

Xia J, Tu K, Yan Z, Qi Y (2016) The super-heat wave in eastern China during July–August 2013: a perspective of climate change. Int J Climatol 36(3):1291–1298. https://doi.org/10.1002/joc.4424

Xu Z, FitzGerald G, Guo Y, Jalaludin B, Tong S (2016) Impact of heatwave on mortality under different heatwave definitions: a systematic review and meta-analysis. Environ Int 89–90:193–203. https://doi.org/10.1016/j.envint.2016.02.007

Yang J, Yin P, Sun J, Wang B, Zhou M, Li M, Tong S, Meng B, Guo Y, Liu Q (2019) Heatwave and mortality in 31 major Chinese cities: definition, vulnerability and implications. Sci Total Environ 649:695–702. https://doi.org/10.1016/j.scitotenv.2018.08.332

You Q, Jiang Z, Kong L, Wu Z, Bao Y, Kang S, Pepin N (2017) A comparison of heat wave climatologies and trends in China based on multiple definitions. Clim Dyn 48(11–12):3975–3989. https://doi.org/10.1007/s00382-016-3315-0

Zampieri M, Russo S, di Sabatino S, Michetti M, Scoccimarro E, Gualdi S (2016) Global assessment of heat wave magnitudes from 1901 to 2010 and implications for the river discharge of the Alps. Sci Total Environ 571:1330–1339. https://doi.org/10.1016/j.scitotenv.2016.07.008

Zhang Q, Singh VP, Peng J, Chen YD, Li J (2012) Spatial–temporal changes of precipitation structure across the Pearl River basin, China. J Hydrol 440–441:113–122. https://doi.org/10.1016/j.jhydrol.2012.03.037

Zhou Y, Ren G (2011) Change in extreme temperature event frequency over mainland China, 1961−2008. Clim Res 50(2):125–139. https://doi.org/10.3354/cr01053

Zhou B, Wen HQZ, Xu Y, Song L, Zhang X (2014) Projected changes in temperature and precipitation extremes in China by the CMIP5 multimodel ensembles. J Clim 27(17):6591–6611. https://doi.org/10.1175/JCLI-D-13-00761.1

Zhou B, Xu Y, Wu J, Shi Y (2016) Changes in temperature and precipitation extreme indices over China: analysis of a high-resolution grid dataset. Int J Climatol 36(3):1051–1066. https://doi.org/10.1002/joc.4400